Copy 5
RM L52I05

NACA RM L52I05

NACA

RESEARCH MEMORANDUM

FOR REFERENCE

AN ANALYSIS OF THE EFFECT OF A CURVED RAMP ON THE TAKE-OFF PERFORMANCE OF CATAPULT-LAUNCHED AIRPLANES

By Wilmer H. Reed, III

Langley Aeronautical Laboratory
Langley Field, Va.

NATIONAL ADVISORY COMMITTEE FOR AERONAUTICS

WASHINGTON

November 5, 1952

NATIONAL ADVISORY COMMITTEE FOR AERONAUTICS

RESEARCH MEMORANDUM

AN ANALYSIS OF THE EFFECT OF A CURVED RAMP ON THE TAKE-OFF PERFORMANCE OF CATAPULT-LAUNCHED AIRPLANES

By Wilmer H. Reed, III

SUMMARY

Some of the newer airplanes designed for carrier operations have high wing loads and wing plan forms with low lift-curve slopes. These configurations may require special catapulting equipment or techniques to prevent an excessive loss of height when catapulted from the deck at a low attitude angle. A curved ramp installed on the deck forward of the catapult release point is considered as a possible solution to this problem. Its function would be to impart an initial upward vertical velocity to provide more time for the controls to pitch the airplane to the required angle of attack before settling could occur and also to impart an initial nose-up pitching velocity so that the development of lift would be more rapid.

An analysis of take-off performance is made by considering a ramp of circular-arc profile 50 feet long with a total rise of 1.73 feet. The assumption that the landing gear is rigid is used throughout the analysis. A straight-wing conventional fighter jet airplane and a low-aspect-ratio delta-wing airplane are used to illustrate the effect of the ramp. Results of flight-path computations are presented for launchings from a straight deck and the curved ramp under conditions of insufficient lift at the instant of take-off. For the case of the straight-deck launchings, the airplanes considered settled from 6 to 9 feet below deck level, whereas for similar launching from the curved ramp there was no tendency to lose altitude.

INTRODUCTION

The design trend of carrier-based jet airplanes is toward high wing loadings and wing plan forms which produce low lift-curve slopes. These characteristics have an adverse effect on the take-off performance of

[redacted]

catapulted airplanes and, for cases in which the ground angle of attack is low, special catapulting devices or procedures may be required to prevent an excessive loss in altitude after the airplane leaves the deck.

Various methods of increasing the angle of attack prior to take-off are under consideration. Among these are

(a) Preloading the nose-wheel oleo strut so that when the catapult bridle is released the nose-wheel restoring force will give the airplane a nose-up pitching acceleration.

(b) Fixing the airplane at a higher-than-normal ground attitude angle by either pumping up the nose-wheel oleo strut or fixing the tail down prior to the catapult power stroke. This procedure introduces problems associated with the inclination of the jet blast such as increased difficulty and hazard to the spotting crew and greater heating of the deck at the catapult starting point. It may also increase the time required for spotting the airplane on the catapult.

(c) Using the catapult force to provide a nose-up pitching acceleration during the power stroke. This procedure might be difficult to control with varying airplane loadings and inconsistencies in the time histories of catapult force. It may also be difficult to obtain an arrangement that is directionally stable during the catapult stroke.

An alternate method of reducing the tendency of the airplane to settle after it leaves the deck is suggested in the present paper. This system incorporates a curved ramp installed on the flight deck forward of the catapult release point. The function of this ramp would be to impart an initial vertical velocity to the catapulted airplane and thereby provide more time for the controls to pitch the airplane to the required angle of attack before settling could occur. In addition, the ramp would, in most cases, provide an initial nose-up pitching velocity which would reduce the time required to pitch to the necessary angle of attack.

Flight-path computations have been made by considering a ramp of circular-arc profile 50 feet long with a total rise of 1.73 feet. With the assumed catapult end speed of 85 knots the upward vertical velocity at the end of the ramp is about 10 feet per second. A conventional straight-wing jet fighter airplane and a low-aspect-ratio delta-wing airplane were used as examples and the calculated take-off chracteristics of these configurations launched from the ramp are compared with similar launchings from a conventional straight deck.

SYMBOLS

A	aspect ratio
a_r	radial acceleration of ramp in g units
$\bar{c}$	wing mean aerodynamic chord
C_D	drag coefficient, D/qS
C_L	lift coefficient, L/qS
C_m	pitching-moment coefficient, $M/qS\bar{c}$
D	drag
e	airplane efficiency factor
F	deck reaction force
g	acceleration due to gravity
h	distance between fuselage reference line and wheel hub measured in plane of symmetry, perpendicular to fuselage reference line
k_Y	radius of gyration about lateral axis
L	lift
l	distance between center of gravity and wheel hub measured in plane of symmetry parallel to fuselage reference line
l'	defined by equation 5 of appendix A
M	pitching moment (positive nose up)
m	airplane mass
q	dynamic pressure $\rho V^2/2$
R	radius of curvature of curved ramp
S	wing area
s	distance relative to air along flight path

t	time
T	thrust
U	wind speed relative to carrier deck
V	true air speed
V_c	catapult end speed relative to deck
W	airplane weight
x	horizontal distance between catapult-bridle release point and main wheel hub
X	axis in direction of free stream
Z	vertical axis perpendicular to free stream
α	angle of attack
δ_e	elevator or elevon angle
θ	attitude angle
μ	coefficient of friction
ρ	air density
γ	flight-path angle
ϕ	deck angle

Subscripts:

n	nose wheel
m	main wheel
t	tail wheel
i	catapult-bridle release point

The terms involving a subscript 0 $\left(C_{L_0},\ C_{D_0}, \text{ and so forth}\right)$ are the values of the coefficients when the variables upon which they depend are zero. A dot over a variable indicates differentiation with respect to time. Definitions of stability derivatives are given by the following

examples:

$$C_{L_\alpha} = \frac{\partial C_L}{\partial \alpha} \qquad C_{m_q} = \frac{\partial C_m}{\partial\left(\frac{\bar{c}\dot{\theta}}{2V}\right)}$$

$$C_{L_{\delta e}} = \frac{\partial C_L}{\partial \delta_e} \qquad C_{m_{D\alpha}} = \frac{\partial C_m}{\partial\left(\frac{\bar{c}\dot{\alpha}}{2V}\right)}$$

METHOD

In order to evaluate the effect of a curved ramp on the take-off performance of catapult-launched airplanes, calculated take-off characteristics of launchings from a curved ramp are compared with launchings from a conventional straight deck. Motion of the airplane was first determined over the interval between the catapult-bridle release point and the end of the deck (a distance of 50 feet). The response of the airplane to conditions which exist at the instant the airplane rolls from the end of the deck was then computed for the early stages of take-off during which the pilot may have little or no control over the airplane's motion. The equations of motion and the computational procedure used for determining the take-off performance are given in appendix A.

The curved ramp.- The curved ramp used as an example in the following calculations is a circular arc with a 720-foot radius which is tangent to and extends 50 feet beyond the catapult release point. The total rise is 1.73 feet and the width is greater than the airplane tread. With a catapult end speed of 85 knots the pitching velocity of an airplane following the curvature of the ramp is 11° per second, the radial acceleration is 0.9g, and the vertical velocity of the wheels at the end of the ramp is 10 feet per second. The geometry and relative size of the ramp and a conventional fighter airplane are shown in figure 1.

Airplanes used as examples.- Two airplanes have been chosen to illustrate the effect of the curved ramp.

Airplane A is a straight-wing fighter airplane with moderate aspect ratio. The physical characteristics and the aerodynamic data obtained from a wind-tunnel test of airplane A are presented in table I. Longitudinal control is provided by elevators mounted on a conventional horizontal tail.

Airplane B is a low-aspect-ratio, tailless configuration with a modified delta-wing plan form. The physical characteristics and wind-tunnel data used in the computations for airplane B are given in table I. Longitudinal control is accomplished by elevons and trimmers located at the trailing edge of the wing. A tail wheel has been added to the tricycle-type landing gear to prevent structural damage to the tail when taking off and landing at high attitude angles. The static attitude angle of this configuration is only 2.7°; however, it is possible to attain 7.0° by pumping the nose-wheel oleo strut to its fully extended position or 14.0° by fixing the airplane in a tail-down position with the tail-wheel oleo strut fully compressed.

Assumed catapult and wind speeds.- Take-off calculations have been carried out by assuming an 85-knot catapult end speed for both airplanes and a wind speed over the deck of 10 knots for the case of airplane A and 25 knots for airplane B. With these airspeeds the lift deficiency on leaving the straight deck was 25 percent for airplane A (attitude angle, 7.4°) and 38 percent for airplane B (attitude angle, 14.0°). A 25-knot wind speed is the minimum normally considered for carrier operations; however, the 10-knot speed was used for airplane A to illustrate the effect of the ramp with this configuration under a critical condition.

RESULTS AND DISCUSSION

Launching characteristics of airplane A.- The computed variations in height, normal acceleration, angle of attack, vertical velocity, true airspeed, and attitude angle with horizontal distance relative to the carrier and referred to the catapult release point are shown in figure 2 for the case of airplane A launched from a straight deck and the curved ramp. An approximate time scale determined from the mean of the velocities in the two cases is also included in figure 2.

In addition to the airplane characteristics listed in table I, airplane A is assumed to have a fixed elevator deflection of -2.0°. With the center-of-gravity location considered (5-percent static margin), this elevator deflection will provide steady trimmed flight at $0.9C_{L_{max}}$. The attitude angle relative to the take-off platform is 7.40° and is the static angle. Since the landing gear is assumed to be rigid and the aerodynamic pitching moment, in this case, is less than the moment required to lift the nose wheel, the attitude angle relative to the deck remains constant until the nose wheel leaves the end of the deck. The airplane then acquires a nose-down pitching acceleration which is sustained until the main wheels leave the end of the deck. Aerodynamic ground effect, which would tend to increase the nose-down pitching acceleration, was neglected for the case of airplane A since its influence on pitching is of such brief duration.

Figure 2 shows that the 10-foot-per-second initial vertical velocity imparted by the ramp is sufficient to prevent the subsequent vertical velocity from becoming negative and the initial pitching velocity has reduced the time required to accelerate upward by about 0.6 second. After the nose wheel leaves the end of the ramp the normal acceleration acting at the center of gravity imposes a nose-down pitching acceleration which tends to reduce the pitching velocity imparted by the ramp. At the time the main wheels leave the end of the ramp the pitching velocity for this case has been reduced from 11.0° to 7.6° per second. The flight path for the straight-deck case dips below deck level a total of 9 feet whereas for the ramp case the airplane remains above deck level and continues to climb. The vertical spread between the flight paths of the two cases at a distance of 500 feet from the end of the deck is about 40 feet.

A pilot may have little control over airplane motion immediately after take-off; therefore consideration should be given to the possibility of exceeding the stall angle of attack caused by the initial pitching velocity imparted by the ramp. Since the angle of attack did not reach the steady-state trim value $\left(0.9C_{L_{max}}\right)$ for which the controls were set throughout the time interval of about 4 seconds covered by the computations, it is apparent that the initial pitching velocity for the case considered is not too great.

Inasmuch as the angle of attack reached by the straight-deck case is less than that for the ramp it is possible that some gain could be realized without danger of overshooting the stall angle by setting the controls for a somewhat higher trim angle of attack for the straight-deck case and thereby increase the pitching acceleration. It is felt, however, that this change would not greatly alter the comparison.

Launching characteristics of airplane B.- A presentation of the take-off characteristics of airplane B launched from a straight deck and the curved ramp is given in figures 3 and 4. The computed variables are the same as those for airplane A in figure 2.

Aerodynamic ground effect as obtained from wind-tunnel test of airplane B in the presence of a ground board is shown in table I. These effects were accounted for in the computations for airplane B prior to leaving the deck and were neglected thereafter. The inclusion of ground effect for the case of airplane B was believed to be necessary since the pitching moment was, for some conditions, sufficient to lift the nose-wheel at the catapult-bridle release point. In such cases the pitching motion is influenced by ground effect over the entire length of the 50 foot take-off run.

Figure 3 shows a comparison of the straight-deck and curved-ramp launchings of airplane B. The control deflection is -9.0° and the

attitude angle at the bridle release point is 7.0°, the angle obtained by blocking out the nose-wheel oleo strut to its fully extended position.

The aerodynamic pitching moment was sufficient to lift the nose wheel during the straight-deck take-off run, but, due to the radial ramp acceleration acting at the center of gravity which is forward of the main wheels, the same aerodynamic pitching moment is insufficient to lift the nose wheel for the case of the curved ramp. As a result, the nose-up pitching velocity at the end of the straight deck is 4.4° per second as compared with 7.0° per second for the curved ramp. Since the difference in nose-up pitching velocity at the instant of take-off is small the potential advantage of the ramp for this case is primarily due to the initial vertical velocity.

The total loss in height following the straight-deck take-off is 6 feet and the airplane remains below deck level for a distance of about 450 feet. The airplane after taking off from the curved ramp continues to climb and, in a distance of 500 feet from the carrier bow, has attained a height 36 feet greater than the straight-deck case. The minimum rates of climb for the case of the curved ramp and straight deck are, respectively, 4 and -8 feet per second.

In figure 4 the ramp launching shown in the preceding figure is compared with a launching from the straight deck in which the initial attitude angle is 14.0° and the control deflection is -15.0°. Also included in the figure are results of computations made for the ramp case in which the control deflection is fixed at -9.0° until the maximum angle of attack is reached at which time the controls are moved in a manner required to hold the angle of attack constant. With the tail-wheel oleo strut fully compressed so that the ground attitude angle is 14.0°, it was assumed that the aerodynamic pitching moment for this case was sufficient to overpower the restoring force of the oleo strut and the tail wheel was considered to be fixed against its stop.

It will be noted from figure 4 that the control deflection for the ramp case is less than that for the straight deck. Computations, the results of which are not shown in figure 4, were also made for the ramp take-off using the same control deflection as was used with the straight-deck launching (-15.0°). These computations showed that the combined effects of pitching acceleration due to the out-of-trim condition and pitching velocity imparted by the ramp along with the low damping in pitch of airplane B caused the angle of attack to reach a peak value of about 30°; this value is believed to be greater than the stall angle of this airplane. It was therefore necessary to use a smaller control deflection for the case of the ramp in the comparisons presented in figure 4. It should be mentioned here that the analysis assumes a linear variation in lift and pitching moment with angle of attack.

Consequently, at large angles of attack where this assumption is no longer an accurate one, the results can only be interpreted qualitatively.

Since the straight-deck case has the higher control setting of the two, as shown in figure 4, the rate of climb for the straight-deck case, when the controls are assumed to remain fixed, will eventually exceed that of the ramp. It is possible, however, for the pilot to improve the rate of climb of the ramp case by increasing the control deflection after there is assurance that the stall angle of attack will not be exceeded. An example is considered wherein the controls are assumed to be fixed at -9.0° until the maximum angle of attack is reached and thereafter are deflected so as to hold the angle of attack constant. This condition could only be approached in the practical case since computations show that the required control motion has the form of a step deflection. The elevon deflection in this case instantaneously changes from -9.0° to -16.9° at the time the angle of attack reaches a maximum value of 24.3°. The deflection then approaches a steady-state value of -16.5°. The computed results using the foregoing assumption are identified in figure 4 by the short dashed curves.

In addition to the results presented herein flight-path computations were also made for airplane B at a lighter weight (17,000 lbs) and at an initial attitude angle of 2.7°. At this angle only 3 percent of the required lift was developed at the end of the deck; however, the initial vertical velocity and the nose-up pitching velocity imparted by the ramp were sufficient to prevent a loss in height due to this lift deficiency at the outset of flight. The minimum vertical velocity in this case was upward 2 feet per second.

CONCLUDING REMARKS

An analysis is made of the effect of a curved ramp installed on a carrier deck forward of the catapult release point for the purpose of improving the take-off performance of catapult-launched airplanes. The ramp under consideration is a circular-arc profile 50 feet long with a total rise of 1.73 feet. The assumption that the landing gear is rigid has been used throughout the analysis.

The results of flight-path computations for a straight-wing conventional fighter jet airplane launched with insufficient lift showed that, in the case of a straight deck, the flight path dipped below deck level a total of 9 feet whereas, for the ramp case, the airplane continued to climb after leaving the ramp. The vertical spread between the flight paths at a distance of 500 feet from the end of the deck is about 40 feet. Similar computations were made for a low-aspect-ratio delta-wing airplane. The total loss in height for this configuration subsequent

to a straight-deck launching was 6 feet and the airplane remained below deck level for a distance of about 450 feet. Settling did not occur for the case of the ramp launching and, in a distance of 500 feet, the height attained was 36 feet greater than the height of the corresponding straight-deck launching.

Langley Aeronautical Laboratory,
National Advisory Committee for Aeronautics,
Langley Field, Va.

APPENDIX A

METHOD OF COMPUTING TAKE-OFF PERFORMANCE

Equations of motion.- The system of moving axis with the origin taken at the airplane center of gravity and the definition of forces and angles are shown in figure 5. A summation of the inertia and external forces and moments acting at the center of gravity when the airplane is in the position indicated by figure 5 produces for the controls-locked case

$$m\dot{V} = T \cos \alpha - D - W \sin \gamma + F_m \left[\sin(\gamma - \phi) - \mu \cos(\gamma - \phi)\right] \tag{A1a}$$

$$mV\dot{\gamma} = L + T \sin \alpha - W \cos \gamma + F_m \left[\cos(\gamma - \phi) + \mu \sin(\gamma - \phi)\right] \tag{A1b}$$

$$Mk_Y{}^2\ddot{\theta} = M - F_m \left[\left(l_m + \mu h_m\right)\cos(\phi - \theta) + \left(h_m - \mu l_m\right)\sin(\phi - \theta)\right] \tag{A1c}$$

The lift, drag, and pitching moment in terms of aerodynamic coefficients are

$$\left.\begin{aligned} L &= qSC_L \\ D &= qSC_D \\ M &= qS\bar{c}C_m \end{aligned}\right\} \tag{A2}$$

where

$$C_L = C_{L_0} + C_{L_{\delta_e}}\delta_e + C_{L_\alpha}\alpha$$

$$C_D = C_{D_0} + \frac{C_L{}^2}{\pi Ae}$$

$$C_m = C_{m_0} + C_{m_{\delta_e}}\delta_e + C_{m_\alpha}\alpha + C_{m_q}\frac{\bar{c}}{2V}\dot{\theta} + C_{m_{D_\alpha}}\frac{\bar{c}}{2V}\dot{\alpha}$$

The terms C_{L_0}, C_{D_0}, and C_{m_0} are the values of the coefficients when the variables upon which they depend are zero. The thrust of turbojet-propelled airplanes is considered constant for the range of speeds involved.

If a tail wheel alone is in contact with the deck the subscript m in equations (A1) is replaced by t and the equations then define the motion after the main wheels leave the end of the deck. When all wheels are clear of the deck, the deck reaction force vanishes and the resulting equations of motion represent the airborne condition.

In order to simplify the analysis, the following general assumptions have been made:

(1) The controls are fixed.

(2) Unsteady lift effects are neglected.

(3) Angular displacements are small.

(4) A linear variation of lift and pitching moment with angle of attack is assumed.

(5) Rolling friction is neglected.

(6) Landing gear is assumed to be rigid.

Airplane motion prior to take-off.- In order to obtain particular solutions of the equations of motion representative of the airborne condition, it is necessary to determine the airspeed, angle of attack, attitude angle, and pitching velocity at the instant the wheels are clear of the deck. When these quantities were computed it was assumed that, during the take-off run, a distance of 50 feet, changes in angle of attack and attitude angle have a negligible effect on acceleration due to thrust and the variations of speed in this region do not affect pitching. Accordingly, the increment in airspeed was determined from equation (A1a) and the angle of attack, attitude angle, and pitching velocity at the end of the deck were found by solving equations (A1b) and (A1c) simultaneously.

It was found convenient to express airspeed in terms of dynamic pressure and to use air distance along the flight path as the independent variable rather than time. For the case of the straight deck, the terms γ and ϕ are zero during the take-off run; therefore, when rolling friction is neglected, equation (A1a) becomes

$$m\dot{V} = \frac{W}{g\rho}\frac{dq}{ds} = T - D$$

If the drag force is assumed to be constant during the take-off run and the substitution

$$s = \frac{V_c + U}{V_c} x$$

is made, the increment in q at the end of the straight deck ($x = 50$) becomes

$$\Delta q = 50\rho g \frac{V_c + U}{V_c} \frac{T - D}{W} \tag{A3}$$

For a corresponding take-off from the curved ramp the increment in q is somewhat less because of the 1.73 feet of height gained. Equating the work required to lift the airplane 1.73 feet to the change in kinetic energy gives

$$\Delta q_{ramp} = 1.73\rho g$$

therefore, at $x = 50$

$$q_{ramp} = q_{straight\ deck} - 1.73\rho g \tag{A4}$$

Rewriting equations (A1b) and (A1c) in accordance with the assumptions of no rolling friction and small angles produces

$$\frac{W}{g} V\dot{\gamma} = L + T\alpha - W + F_m \tag{A5a}$$

$$\frac{W}{g} k_Y^2 \ddot{\theta} = M - F_m l'_m \tag{A5b}$$

where

$$l'_m = l_m + h_m(\phi - \theta)$$

The difference in the local deck angle and the airplane attitude angle, $\phi - \theta$, is practically constant during the take-off; therefore l'_m may be satisfactorily approximated by its value at $x = 0$

$$l'_m = l_m - h_m\theta_i$$

It will be noted that equations (A5) apply for the case in which the nose wheel is not touching the deck. Since the landing gear is assumed to be rigid, this condition exists whenever the aerodynamic pitching moment during take-off is sufficient to produce a nose-up pitching acceleration or when the nose wheel rolls from the end of the deck. In the case with the nose wheel in contact with the deck the motion of the airplane before the nose wheel reaches the end of the deck (straight or with ramp) is defined purely by the geometry of the take-off platform.

The normal acceleration at the center of gravity in g units may be expressed in terms of the radial acceleration of the ramp by the relation

$$\frac{V}{g}\dot{\gamma} = a_r + \frac{l'_m}{g}\ddot{\theta} \tag{A6}$$

where

$$a_r = \frac{V_c^2}{gR}$$

When F in equations (A5) is eliminated and the resulting equations is combined with equation (A6) the pitching acceleration becomes

$$\ddot{\theta} = \frac{g}{(l'_m)^2 + k_Y^2}\left[\left(\frac{L + T\alpha}{V} - a_r - 1\right)l'_m + \frac{M}{W}\right] \tag{A7}$$

The angle-of-attack change during the take-off run was small and, as a consequence, changes in the lift and pitching moment in this region were neglected. The pitching acceleration given by equation (A7) was therefore assumed to be constant over the region in which the nose wheel was free of the deck.

The values of α, θ, and $\frac{d\theta}{ds}$ at the instant the main wheels leave the deck ($x = 50$) may be computed from the following relations:

$$\left.\begin{aligned}
\theta &= \theta_0 + \dot{\theta}_0\,\Delta t + \frac{1}{2}\,\ddot{\theta}_0\,\Delta t^2 \\
\frac{d\theta}{ds} &= \frac{1}{V_c + U}\left(\dot{\theta}_0 + \ddot{\theta}_0\,\Delta t\right) \\
\alpha &= \theta - \gamma \\
&= \theta - \frac{V_c\,\frac{50}{R} + l'_m\left(\dot{\theta}_0 + \ddot{\theta}_0\,\Delta t\right)}{V_c + U}
\end{aligned}\right\} \qquad \text{(A8)}$$

The term θ_0 and its derivatives are evaluated at x_0, the distance between the bridle release point and the main wheels at the time the nose wheel leaves the deck. When these quantities are expressed in terms of the deck geometry, they may be written

$$\theta_0 = \theta_i + \frac{x_0 + \frac{l_m + l_n}{2}}{R}$$

$$\dot{\theta}_0 = \frac{V_c}{R}$$

$$\ddot{\theta}_0 = F\left(\alpha_0,\ \delta_e,\ R,\ V_c,\ U\right)$$

where

$$\alpha_0 = \theta_0 - \frac{V_c\left(X_0 + l'_m\right)}{R(V_c + U)}$$

and the aerodynamic damping in pitch is neglected.

When the pitching acceleration $\ddot{\theta}$ evaluated at the bridle release point is positive (nose up) the nose wheel lifts at $x = 0$ and Δt in equation (A8) is given the value $\frac{50}{V_c}$. When the pitching acceleration is equal to or less than zero at the bridle release point the nose wheel remains in contact with the deck until $x = 50 - \left(l_n + l_m\right)$ in which case $\Delta t = \frac{l_n + l_m}{V_c}$.

[redacted]

The quantities q, θ, α, and $\frac{d\theta}{ds}$ evaluated at the end of the deck by the preceding approximate relations (eqs. (A3), (A4), and (A8)) were found to be in good agreement with an analytical solution of a linearized form of equation (A1) in which the variations of lift, drag, and pitching moment during the take-off run were accounted for.

Airplane motion after take-off.- In the absence of the deck reaction force, equations (A1) define airplane motion for the airborne condition. When it is noted that $\gamma = \theta - \alpha$, equations (A1) and (A2) combine to yield three simultaneous differential equations where the unknown variables are q, α, and θ. These equations are as follows:

$$\left.\begin{aligned}
\frac{dq}{ds} &= a_1 + q\left(a_2 + a_3\alpha + a_4\alpha^2\right) + a_5(\theta - \alpha) \\
\frac{d\alpha}{ds} &= a_6 + \frac{d\theta}{ds} + a_7\alpha + \frac{1}{q}\left(a_8 + a_9\alpha\right) \\
\frac{d^2\theta}{ds^2} &= a_{10} + a_{11}\alpha + a_{12}\frac{d\theta}{ds} + a_{13}\frac{d\alpha}{ds} + \frac{a_{19}}{q}\frac{dq}{ds}\frac{d\theta}{ds}
\end{aligned}\right\} \qquad \text{(A9)}$$

in which

$$a_1 = \frac{\rho T}{m}$$

$$a_2 = \frac{-\rho S}{m}\left(C_{D_0} + \frac{C_{L_0} + C_{L_{\delta_e}}\delta_e}{\pi A_e}\right)$$

$$a_3 = \frac{\rho S}{m}\,\frac{2C_{L_\alpha}\left(C_{L_0} + C_{L_{\delta_e}}\delta_e\right)}{\pi A_e}$$

$$a_4 = -\frac{\rho S}{m}\,\frac{C_{L_\alpha}{}^2}{\pi A e}$$

$$a_5 = -\frac{\rho W}{m}$$

$$a_6 = -\frac{\rho S\left(C_{L_0} + C_{L_{\delta_e}}\delta_e\right)}{2m}$$

$$a_7 = -\frac{\rho S C_{L_\alpha}}{2m}$$

$$a_8 = \frac{\rho W}{2m}$$

$$a_9 = -\frac{\rho T}{2m}$$

$$a_{10} = \frac{\left(C_{m_0} + C_{m_{\delta_e}}\delta_e\right)\rho S\bar{c}}{2mk_Y^2}$$

$$a_{11} = \frac{C_{m_\alpha} S\bar{c}\rho}{2mk_Y^2}$$

$$a_{12} = \frac{C_{m_q}\rho S\bar{c}^2}{4mk_Y^2}$$

$$a_{13} = \frac{C_{m_{D\alpha}}\rho S\bar{c}^2}{4mk_Y^2}$$

$$a_{14} = \frac{1}{2}$$

Equations (A9), subject to the initial conditions q, α, θ, and $\frac{d\theta}{ds}$ evaluated at the point where the airplane leaves the deck, were integrated on the Bell Telephone Laboratories X-66744 relay computer at the Langley Laboratory by using the Runge-Kutta numerical method. A description of this step-by-step procedure for solving simultaneous differential equations may be found in reference 1.

REFERENCE

1. Scarborough, James B.: Numerical Mathematical Analysis. The Johns Hopkins Press (Baltimore), 1930, pp. 299-303.

TABLE I

CHARACTERISTICS OF AIRPLANES USED IN CALCULATIONS

Characteristic	Airplane A	Airplane B
W, lb	13,000	19,000
m, slugs	403.9	590.0
k_Y, ft	6.68	7.30
V_c, knots	85	85
U, knots	10	25
T, lb	5,000	8,000
S, sq ft	260	557
A	4.80	2.02
$\bar{c}$, ft	7.45	18.25
Center-of-gravity location, percent mean aerodynamic chord	25.5	22.0
l_m, ft	1.5	1.9
h_m, ft	3.1	5.2
l_t, ft	------	12.0
h_t, ft	------	2.8
l_n, ft	12.0	14.3

TABLE I.- Concluded

CHARACTERISTICS OF AIRPLANES USED IN CALCULATIONS

Characteristic	Airplane A	Airplane B	
	Without ground effect	Without ground effect	With ground effect
C_{L_0}	0.53	-0.11	-0.22
C_{L_α}, per radian	4.27	2.64	3.67
$C_{L_{\delta_e}}$, per radian	0.57	0.49	0.52
C_{D_0}	0.11	0.00[a]	0.040
e	0.735	0.422	0.830
C_{m_0}	0.028	0.058	0.103
$\frac{dC_m}{dC_L}$	-0.050	-0.120	-0.164
C_{m_α}, per radian	-0.214	-0.316	-0.565
$C_{m_{\delta_e}}$, per radian	-1.080	-0.271	-0.291
C_{m_q}	-12.70	-0.70	-0.70
$C_{m_{D\alpha}}$	-5.08	0	0

[a]The experimental variation of C_D with C_L^2 was nonlinear and had a value of C_{D_0} of 0.04. The closest linear approximation to the experimental data, particularly at the higher lift coefficients, involved using a value of C_{D_0} of zero.

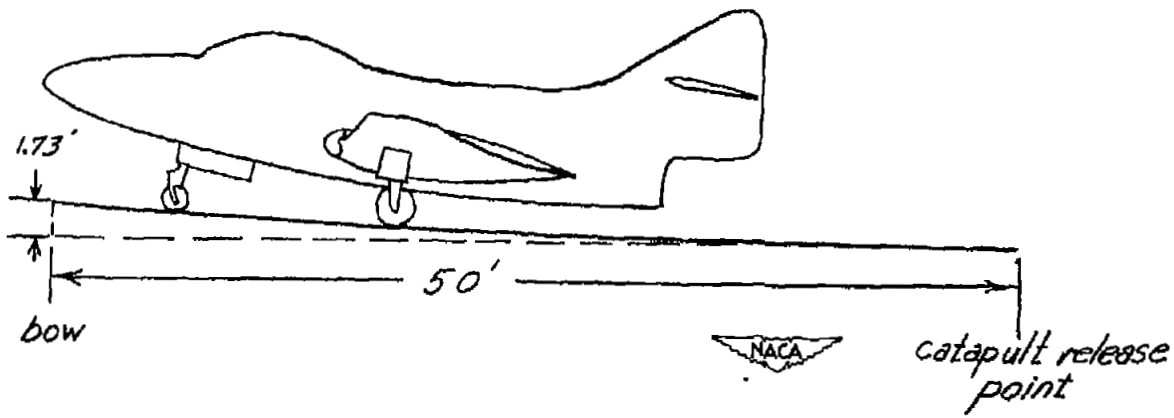

Figure 1.- Geometry and relative size of the circular-arc ramp and a conventional fighter airplane.

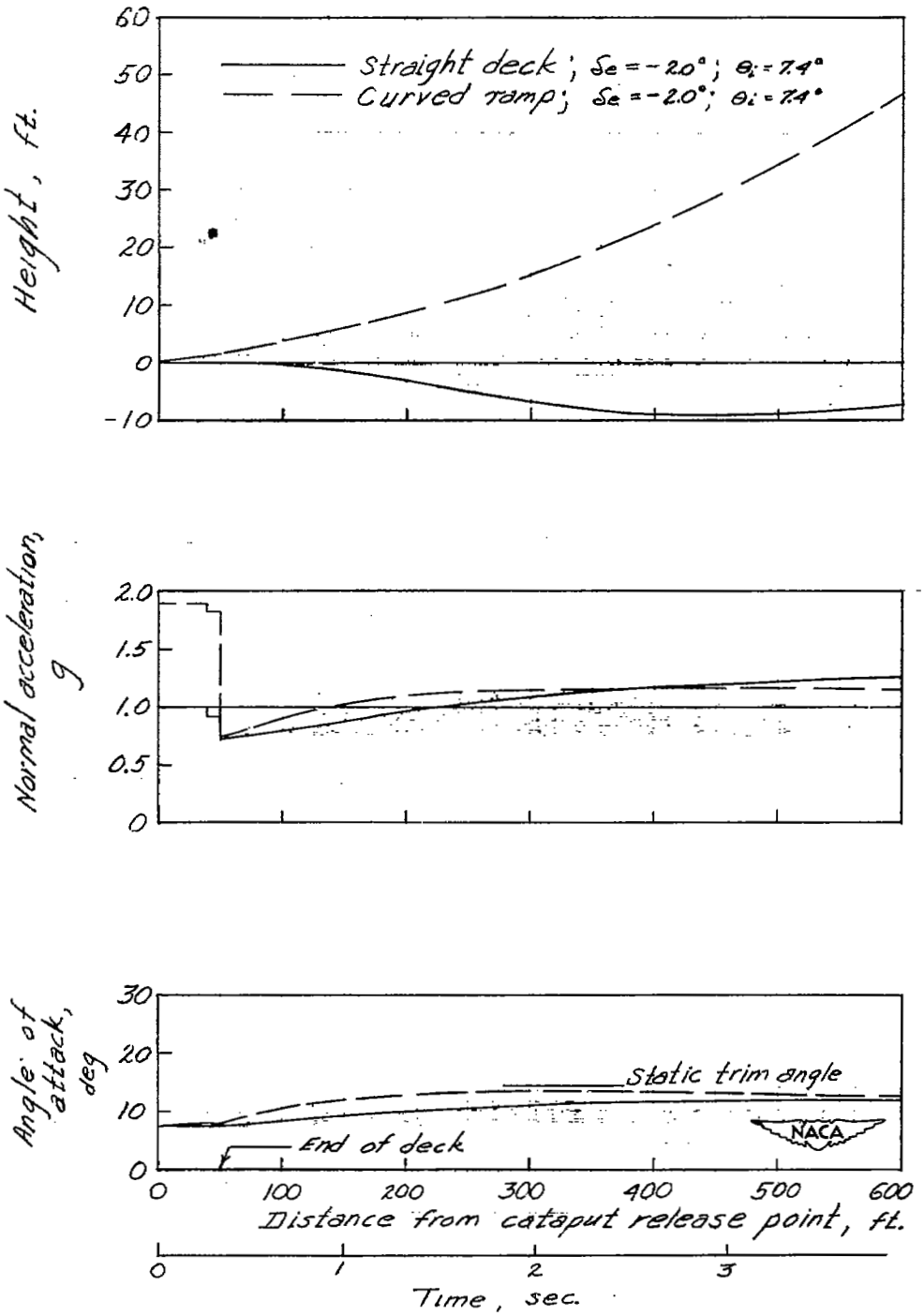

Figure 2.- Calculated take-off characteristics of airplane A. $\delta_e = -2.0°$ and $\theta_i = 7.4°$ for the straight deck and curved ramp.

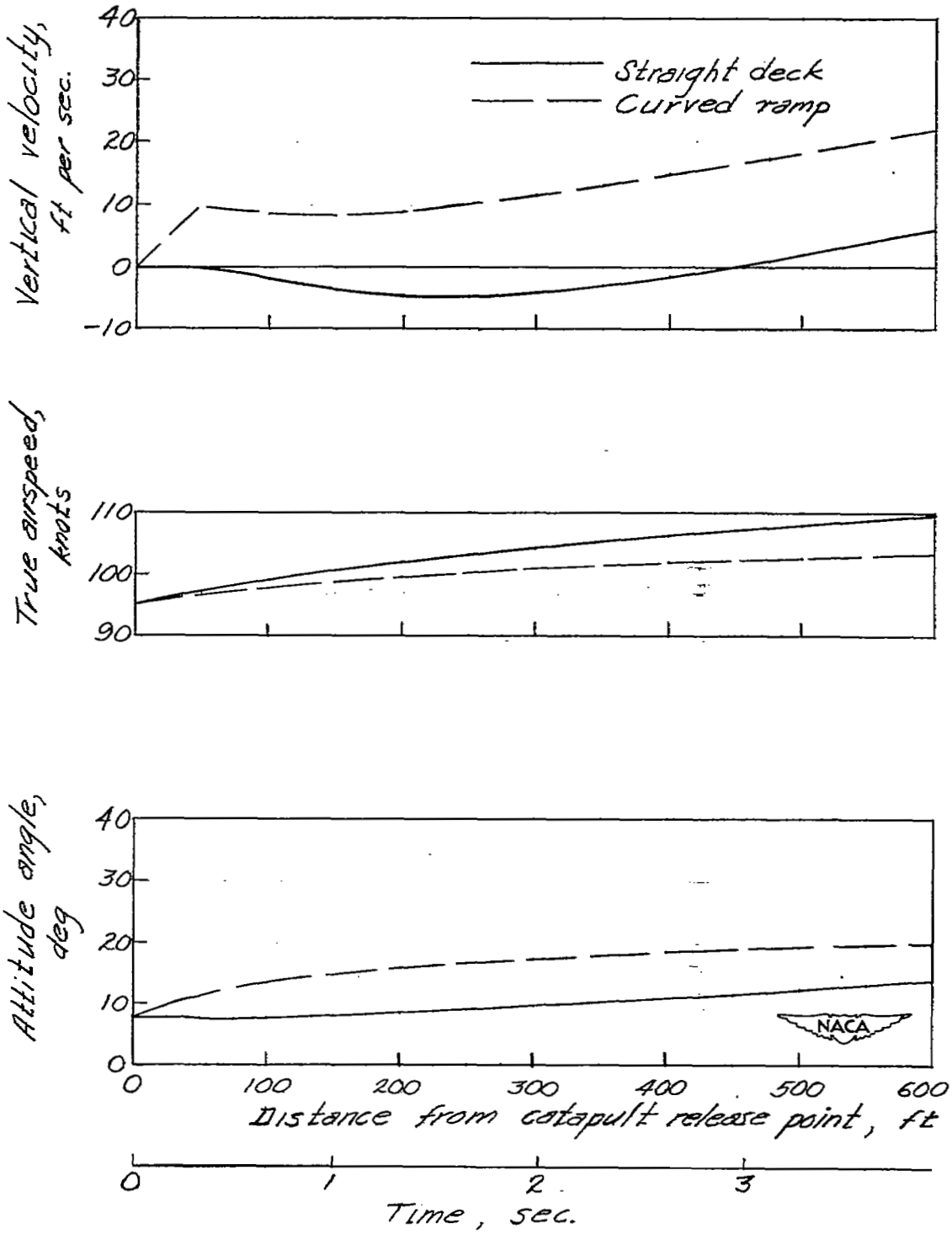

Figure 2.- Concluded.

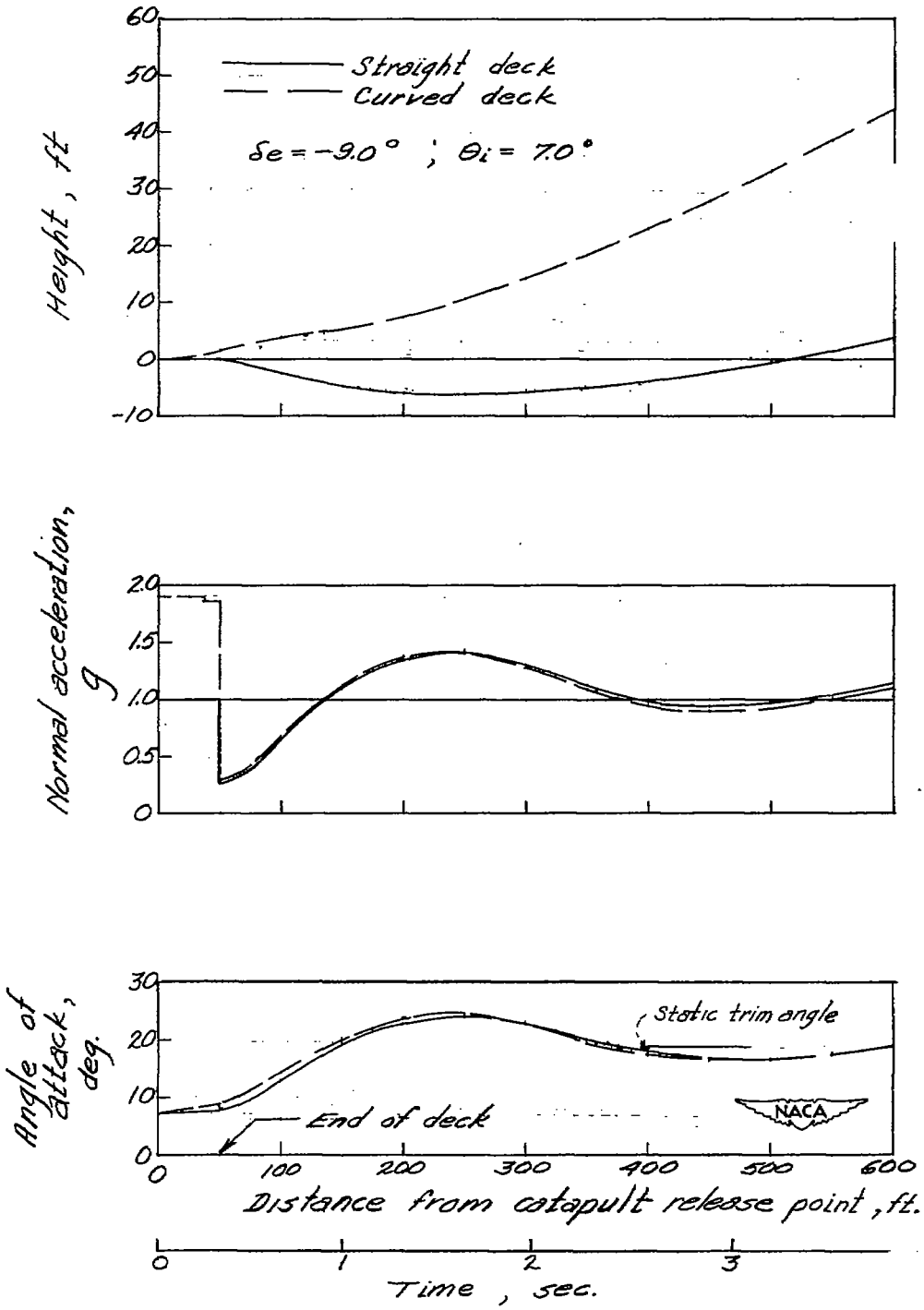

Figure 3.- Calculated take-off characteristics of airplane B. $\delta_e = -9.0°$ and $\theta_i = 7.0°$ for the straight deck and curved ramp.

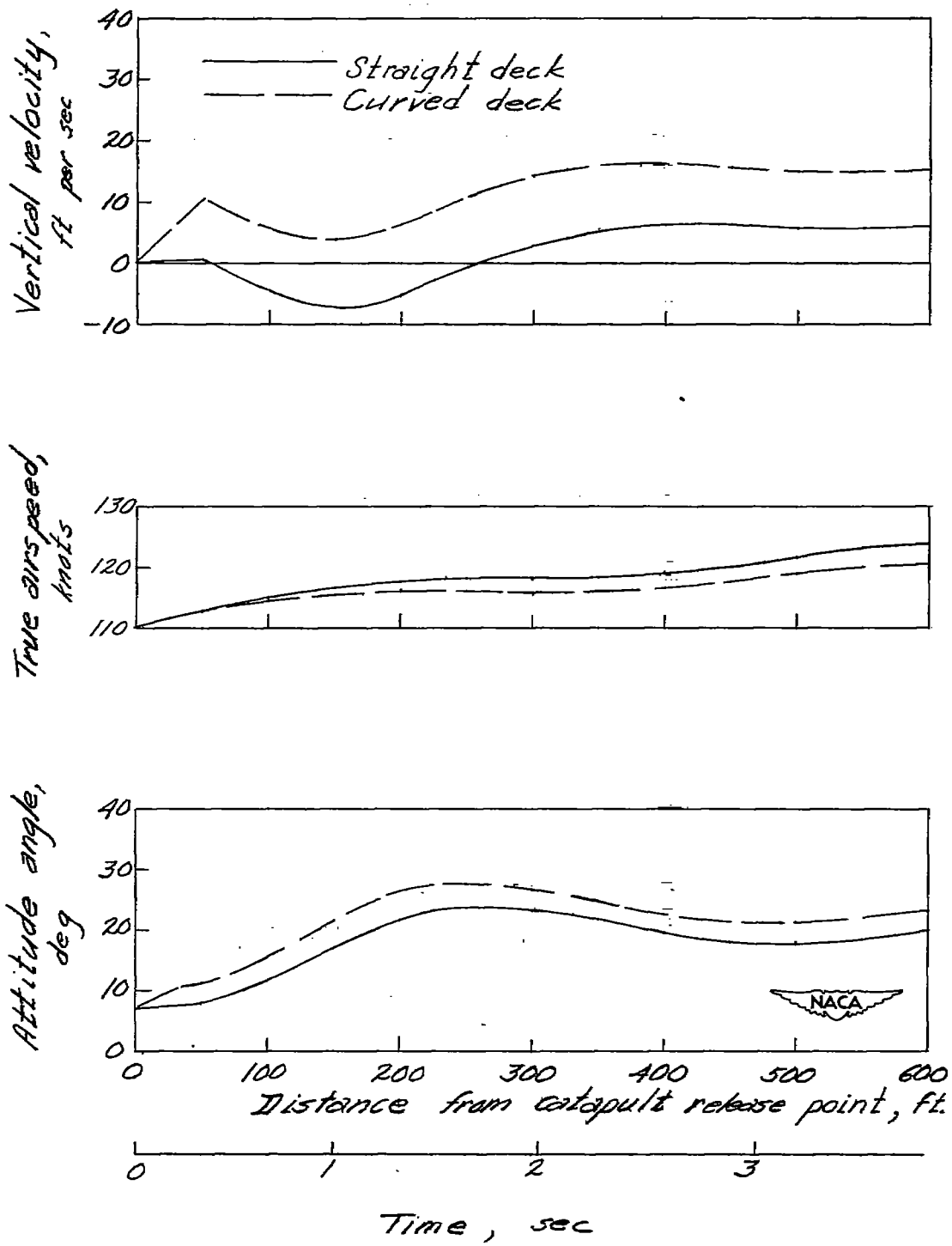

Figure 3.- Concluded.

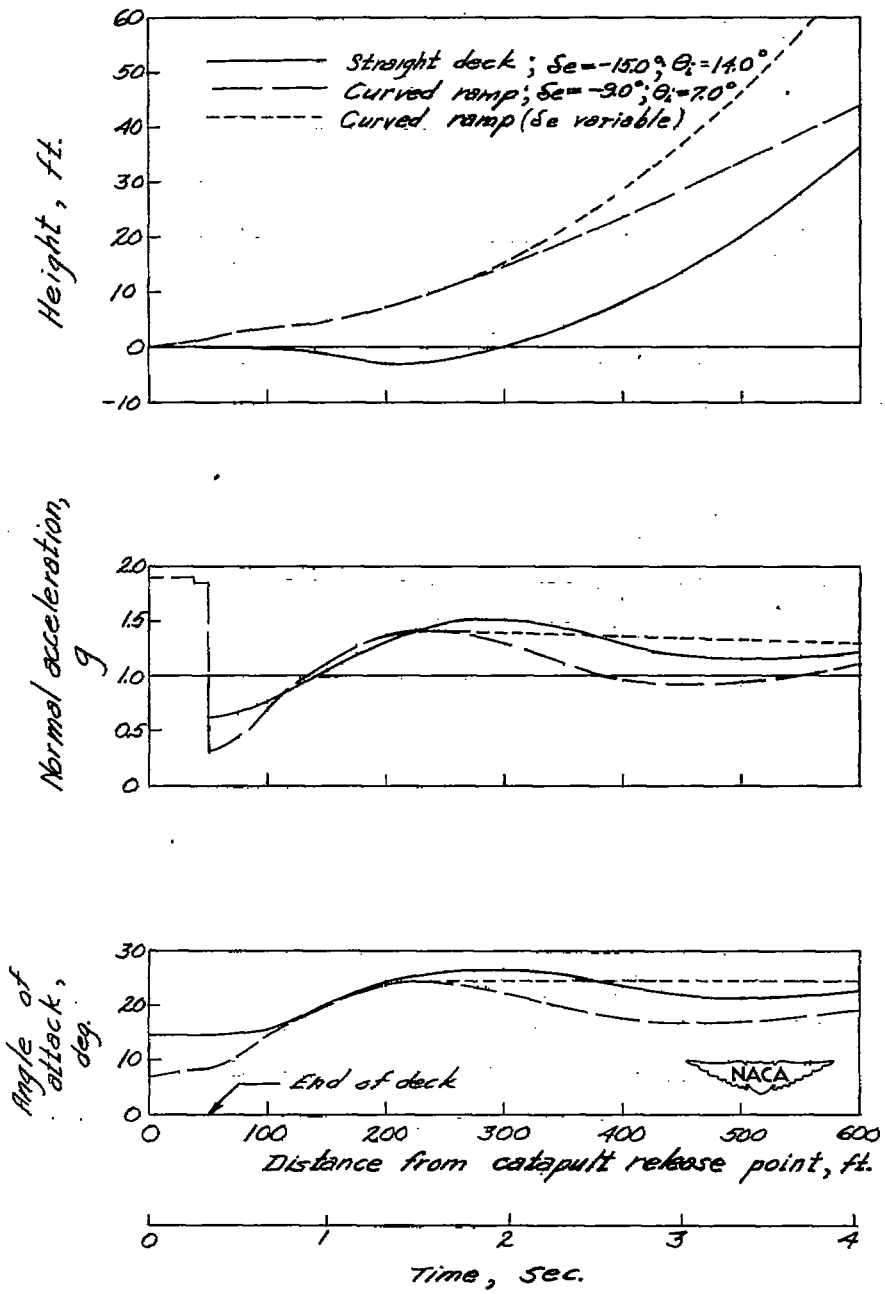

Figure 4.- Calculated take-off characteristics of airplane B. $\delta_e = -15.0^\circ$ and $\theta_i = 14.0^\circ$ for the straight deck and $\delta_e = -9.0^\circ$ and $\theta_i = 7.0^\circ$ for curved ramp. Also shown is the case where the control deflection is varied so that the angle of attack remains constant at its peak value.

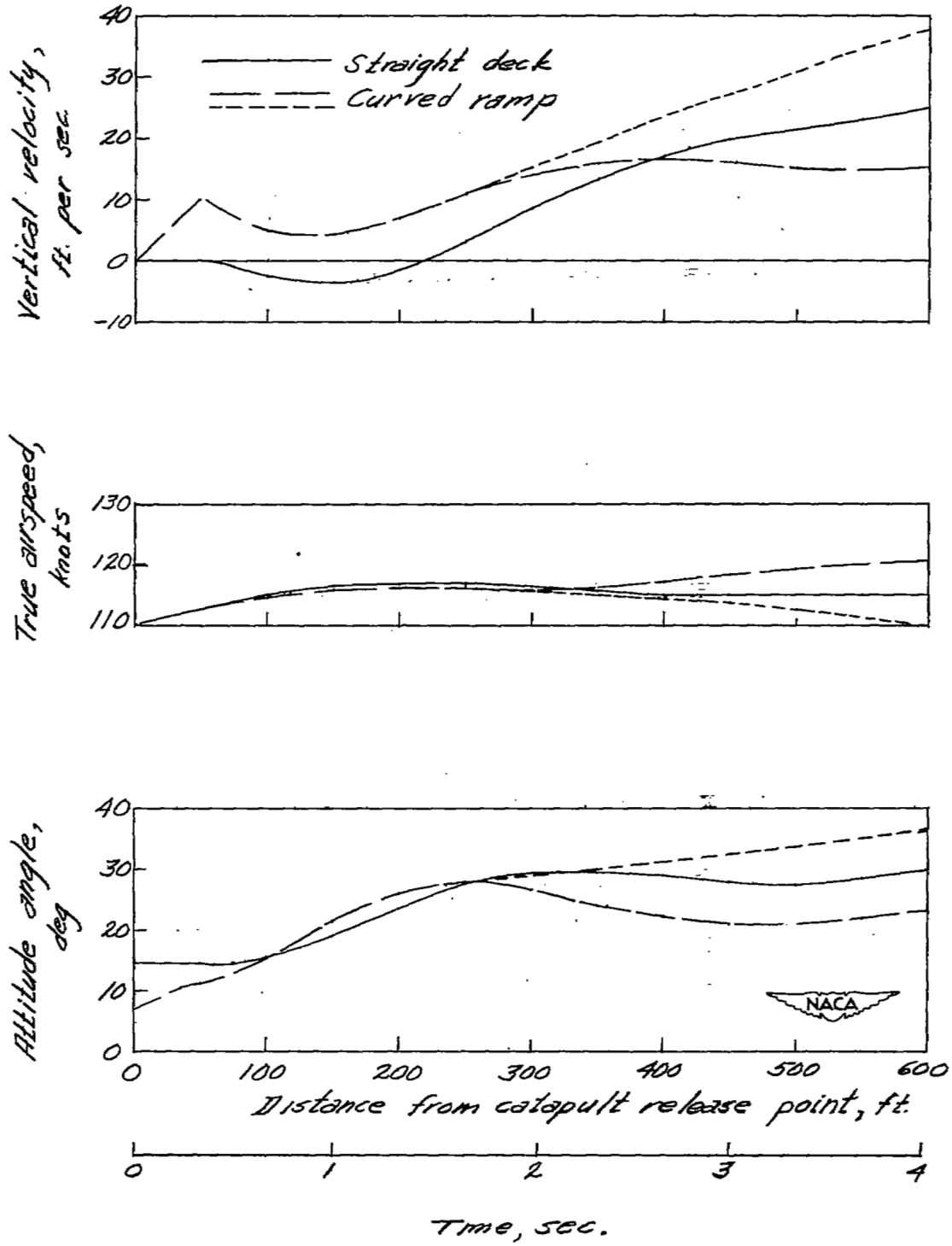

Figure 4.- Concluded.

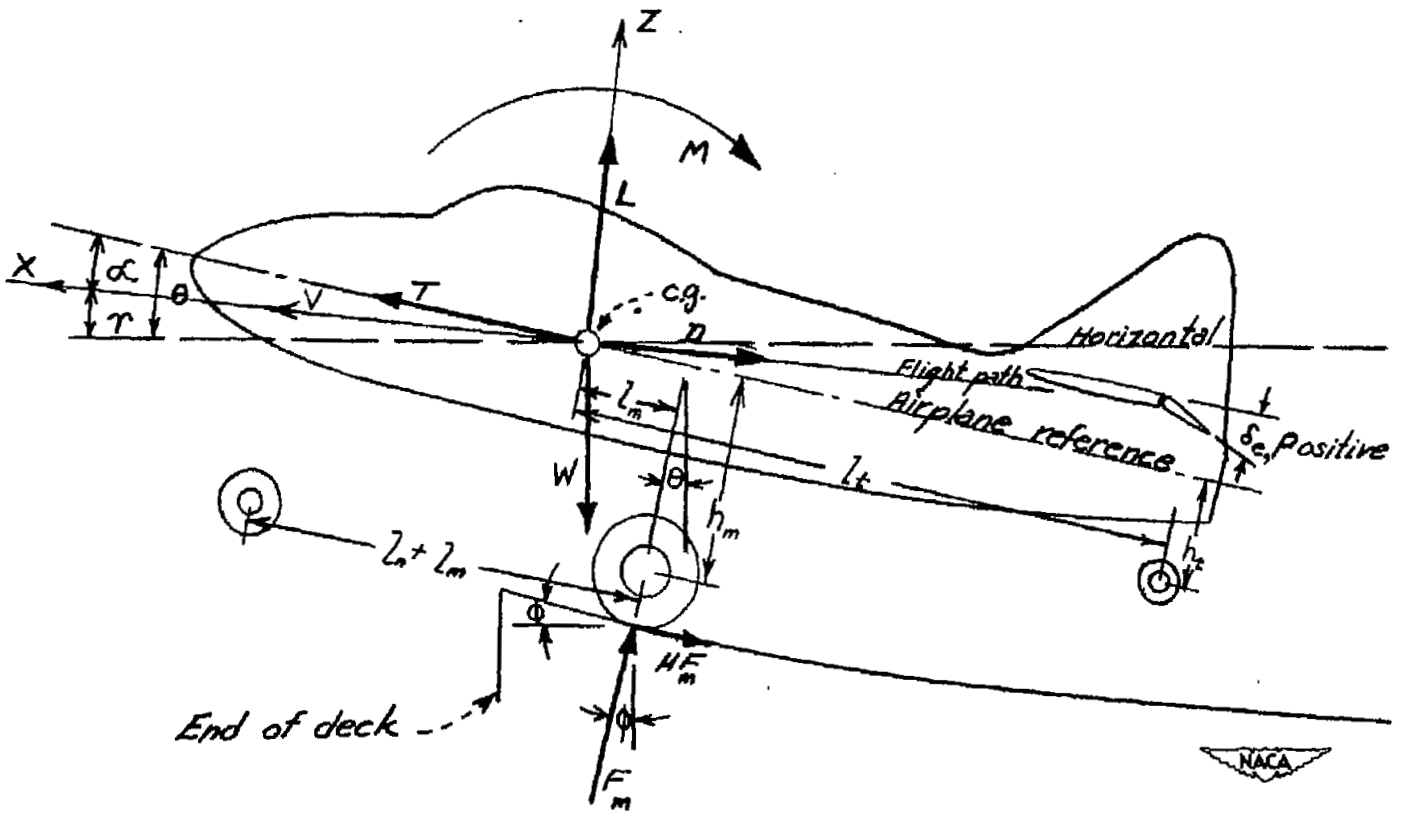

Figure 5.- Forces and moments acting on a catapult-launched airplane when the main wheels are in contact with the deck.